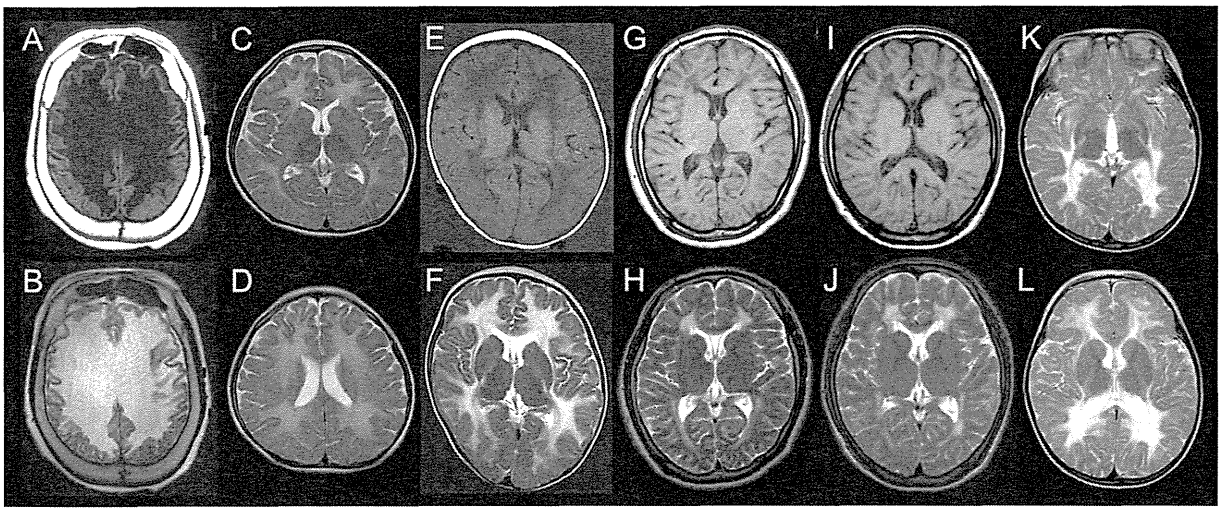

Fig. 1. Brain MRI findings of the patients examined. Axial images show various degrees of abnormal white matter. (A and B) Patient 1 examined at 60 years of age. (C and D) Patient 2 examined at 3 years of age. (E and F) Patient 3 examined at 8 months of age. (G and H) Patient 4 examined at 13 years of age. (I and J) Patient 5 examined at 16 years of age. (K and L) Patient 6 examined at 13 months of age. T1-weighted axial images (A, E, G, and I) and T2-weigthed axial images (B–D, F, H, and J–L). Periventricular zones of patient 1 are not distinguished (A and B). T2-high intensity is only shown in deep white matter, indicating early disease stage in patient 4 and 5 (H and J, respectively).

intensity in the white matter (Fig. 1). Routine laboratory examinations of blood, urine, and CSF showed no abnormality. Her neurological findings have gradually improved. At present, she can speak simple sentences and can walk unassisted.

Patient 3, a baby boy, was born with a weight of 2878 g (25th–50th centile), a length of 49.4 cm (50th–75th centile), and occipitofrontal circumference (OFC) of 33.0 cm (25th–50th centile) at 41 weeks of gestation. At 6 months of age, he showed postnatal growth delay with a weight of 6.2 kg (<3rd centile), a length of 63.4 cm (3rd–10th centile), and OFC of 42 cm (10th–25th centile). Although he showed normal development until 8 months of age, he suddenly displayed drowsiness and poor sucking after an infectious disorder causing high fever, and was admitted to the hospital. At that time, the brain MRI showed diffuse T2 high intensity in the white matter (Fig. 1). Routine laboratory examinations of blood, urine, and CSF, including lactate and pyruvate, showed no abnormality. Screening tests for metabolic disorders of amino acids and very long chain fatty acids also appeared normal. Thereafter, he showed spasticity and severe developmental delay.

Patient 4 is a 22-year-old male, first born from non-consanguineous parents. At the age of 13 years, he started to show epileptic seizures. At that time, brain MRI showed diffuse T2 high intensity in the white matter. Screening tests for metabolic disorders of amino acids and very long chain fatty acids showed normal patterns in patient 4. Enzyme activity of arylsulfatase A and β-galactosidase as well as peripheral nerve conduction velocities, were all within the normal limit. At present, he only shows mild ataxia. Patient 5, the 19-year-old younger brother of patient 4, is the third born among three siblings; his elder sister (the second born) is healthy. Patient 5 also showed a clinical course similar to that of patient 4; he showed epileptic seizures and brain MRI abnormality at age 13 years. When he was 16 years old, a traumatic accident triggered disease progression; he showed prolonged delirium, and then muscular weakness in his left side. Routine laboratory examinations of blood, urine, and CSF showed no abnormality in this sibling case.

Patient 6 is a 3-year and 5-month-old boy. There was no remarkable family or past history. At 13 months, he showed transient drowsiness and gait disturbance two weeks after a febrile convulsion. Brain MRI showed T2 high intensity in the white matter (Fig. 1). After 2 years of age, he easily dropped due to ataxic gait. At present, his height is 95.1 cm (25th–50th centile), weight is 15.9 kg (75th–90th centile), and OFC is 51.8 cm (90th–97th centile). He cannot stand alone due to spasticity in his lower extremities. Compared to motor development, his cognitive development was within the normal limit. Screening tests for metabolic disorders of amino acids and very long chain fatty acids showed normal patterns. Enzyme activities including arylsulfatase A, β-hexosaminidase A, β-galactosidase, galactosylceramidase were within the normal limits. There were no mutations in the glial fibrillary acidic protein gene (*GFAP*) nor the megalencephalic leukoencephalopathy with subcortical cysts 1 gene (*MLC1*).

4. Discussion

In this study, a molecular diagnosis of VWM was established in six patients from five families (Table 1). All of the identified mutations are depicted in the

primary structures of EIF2B genes together with previously reported mutations (Fig. 2) [4–16]. The damage prediction scores of the identified mutations were calculated and summarized in Table 1. Although the some of the predictions from SIFT and Polyphen-2 appeared benign or tolerated, all CADD scores (PHRED-like) were higher than 15. Thus, mutations identified in this study likely to have pathogenic effects.

In patient 6, p.I385T was inherited from his mother; however, p.M305I was not identified either parent. Therefore, p.M305I was suspected to be of *de novo* origin in the paternally derived allele. The UCSC Genome Bioinformatics Site displays the different single nucleotide polymorphisms (SNPs) in the same residues, p.M305L (rs200143780) and p.I385V (rs113994073) (Supplemental Fig. 2). The p.I385V is registered as a "flagged" SNP and has previously been reported as pathogenic [24] (Fig. 2). Compared to this, p.M305L is not shown as a "flagged" in the database; however, the minor allele frequency (MAF) of p.M305L is reported to be as low as 0.050% (1/2000). Because VWM is caused by an autosomal recessive trait, existence of only one individual with heterozygosity of p.M305L among 1000 normal populations may suggest that this individual is a healthy carrier of this possibly disease-causing variant. Therefore, existence of the different SNP of this residue (p.M305L) in the database does not deny pathogenesis of p.M305I. These findings indicate that these two variants are likely deleterious.

Among the 10 alleles present in the five families, three alleles (30%) shared the p.V85E mutation in *EIF2B2*. Previously, p.V85E has been identified in Japanese

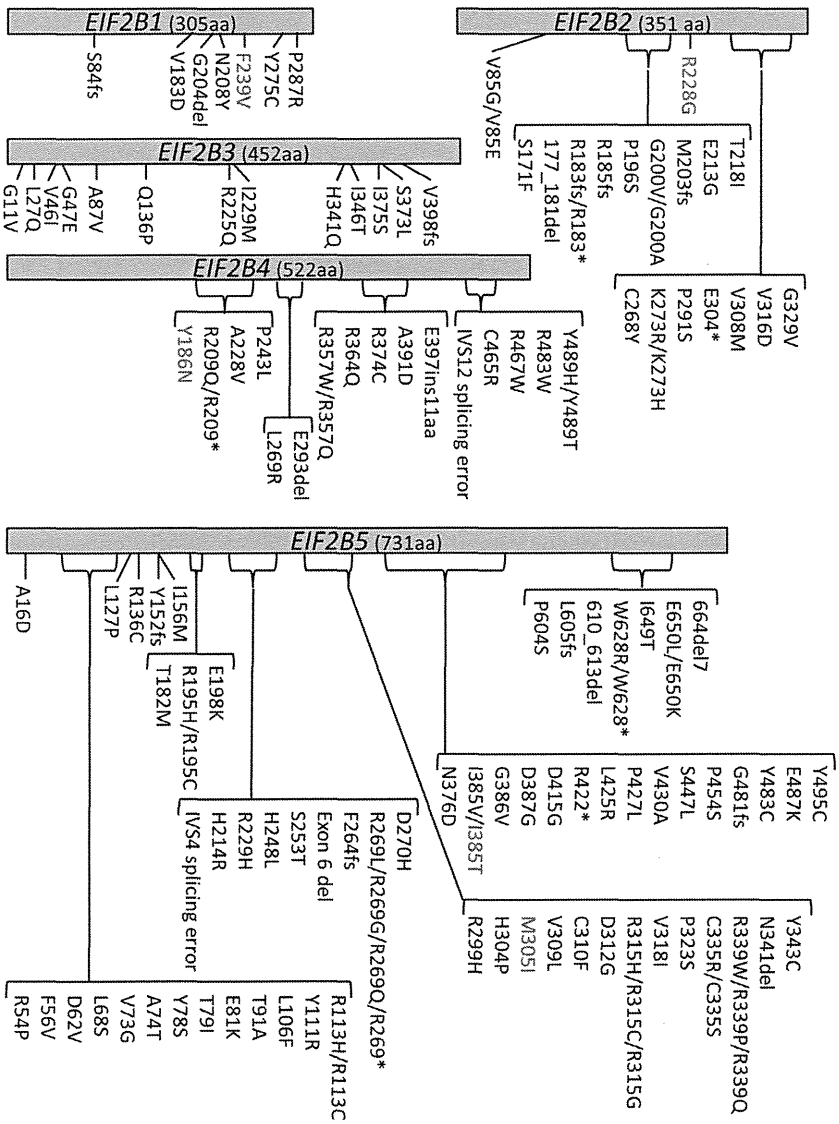

Fig. 2. Schematic representation of the distribution of EIF2B gene mutations. The novel mutations identified in this study are depicted on the primary structures of EIF2B genes in red characters, while known mutations are shown in black. (For interpretation of the references to color in this figure legend, the reader is referred to the web version of this article.)

patients [25]. We also reported this mutation in a patient with VWM, which was unmasked by a microdeletion of the homologous allele [26]. Therefore, this mutation is most common in the Japanese population. Because p.V85E has also identified in a Chinese patient [13], this variant may be common in individuals of east Asian origin. Other than p.V85E in *EIF2B2*, p.R357Q in *EIF2B4*, registered as rs113994033, was recurrently identified in the literature [8]. The other five mutations identified in this study were novel and have not been reported previously (Table 1). Due to the limited number of patients, we were unable to identify any genotype–phenotype correlation.

In this study, patient 1 at 61 years of age presented clinical manifestations of the end stage of VWM, with completely vanishing white matter. We are unable to distinguish the border of periventricular zones in the brain MRI for this patient. Although patient 1 is now bedridden with no response or motor activity, the onset of her neurological symptoms began at age 29. Therefore, compared to the other patients, this patient showed later onset of disease and slower disease progression. The sibling case of patient 4 and 5 also showed late onset and slow progression, and only started to exhibit neurological symptoms after adolescence. In the early stage of VWM, brain MRI may not necessarily show diffuse cerebral white matter abnormalities and rarefaction or cystic degeneration [27]. Therefore, the brain MRI of patient 4 and 5, showing abnormal T2 high intensity only in the deep white matter, is suggestive of an early disease stage.

The other three patients (patient 2, 3, and 6) showed typical, diffuse white matter abnormalities in MRI. They started to show neurological symptoms during early infancy, and their disease occurrences were triggered by environmental factors (high fever due to infections) and were followed by episodes of acute deterioration associated with disturbed consciousness and seizures. These provocations have been frequently observed in VWM patients [11].

Because EIF2B is involved in regulating the first steps of protein synthesis and is ubiquitously expressed, it is unclear why EIF2B alterations cause a brain-specific disease [28,29]. Although many mutations identified in patients with VWM showed reduced EIF2B activities [30], basal activities *per se* do not explain the disease severity. Rather, the decreased EIF2B activity might impair the cellular stress response and improperly activate the unfolded protein response (UPR) leading to the endoplasmic reticulum (ER) stress [31]. The ER load in astrocytes and oligodendrocytes is possibly higher than in other cell types, rendering them vulnerable to conditions that predispose to ER stress [32,33]. This is the probable reason for disease provocations after environmental stress factors in patients with EIF2B alterations.

In this study, we recruited 22 patients who showed mimicking clinical manifestations of VWM. Among them, only six patients had genomic mutations in EIF2B genes. The final diagnosis of the other 16 patients is unknown at present. This would be challenges to be overcome in our future.

Acknowledgements

We would like to acknowledge the Collaborative Research Supporting Committee of the Japanese Society of Child Neurology (14-3) for promoting this study. This work was supported by a Grant-in-Aid for Scientific Research from Health Labor Sciences Research Grants from the Ministry of Health, Labor, and Welfare, Japan (T.Y.).

Appendix A. Supplementary data

Supplementary data associated with this article can be found, in the online version, at http://dx.doi.org/10.1016/j.braindev.2015.03.003.

References

[1] van der Knaap MS, Barth PG, Gabreels FJ, Franzoni E, Begeer JH, Stroink H, et al. A new leukoencephalopathy with vanishing white matter. Neurology 1997;48:845–55.
[2] Hanefeld F, Holzbach U, Kruse B, Wilichowski E, Christen HJ, Frahm J. Diffuse white matter disease in three children: an encephalopathy with unique features on magnetic resonance imaging and proton magnetic resonance spectroscopy. Neuropediatrics 1993;24:244–8.
[3] Schiffmann R, Moller JR, Trapp BD, Shih HH, Farrer RG, Katz DA, et al. Childhood ataxia with diffuse central nervous system hypomyelination. Ann Neurol 1994;35:331–40.
[4] Leegwater PA, Vermeulen G, Konst AA, Naidu S, Mulders J, Visser A, et al. Subunits of the translation initiation factor eIF2B are mutant in leukoencephalopathy with vanishing white matter. Nat Genet 2001;29:383–8.
[5] van der Knaap MS, Leegwater PA, Konst AA, Visser A, Naidu S, Oudejans CB, et al. Mutations in each of the five subunits of translation initiation factor eIF2B can cause leukoencephalopathy with vanishing white matter. Ann Neurol 2002;51:264–70.
[6] Pronk JC, van Kollenburg B, Scheper GC, van der Knaap MS. Vanishing white matter disease: a review with focus on its genetics. Ment Retard Dev Disabil Res Rev 2006;12:123–8.
[7] Maletkovic J, Schiffmann R, Gorospe JR, Gordon ES, Mintz M, Hoffman EP, et al. Genetic and clinical heterogeneity in eIF2B-related disorder. J Child Neurol 2008;23:205–15.
[8] Scali O, Di Perri C, Federico A. The spectrum of mutations for the diagnosis of vanishing white matter disease. Neurol Sci 2006;27:271–7.
[9] Matsui M, Mizutani K, Ohtake H, Miki Y, Ishizu K, Fukuyama H, et al. Novel mutation in EIF2B gene in a case of adult-onset leukoencephalopathy with vanishing white matter. Eur Neurol 2007;57:57–8.
[10] Horzinski L, Gonthier C, Rodriguez D, Scherer C, Boespflug-Tanguy O, Fogli A. Exon deletion in the non-catalytic domain of eIF2Bepsilon due to a splice site mutation leads to infantile forms of CACH/VWM with severe decrease of eIF2B GEF activity. Ann Hum Genet 2008;72:410–5.

[11] Labauge P, Horzinski L, Ayrignac X, Blanc P, Vukusic S, Rodriguez D, et al. Natural history of adult-onset eIF2B-related disorders: a multi-centric survey of 16 cases. Brain 2009;132:2161–9.
[12] Wu Y, Pan Y, Du L, Wang J, Gu Q, Gao Z, et al. Identification of novel EIF2B mutations in Chinese patients with vanishing white matter disease. J Hum Genet 2009;54:74–7.
[13] Leng X, Wu Y, Wang X, Pan Y, Wang J, Li J, et al. Functional analysis of recently identified mutations in eukaryotic translation initiation factor 2Bε (eIF2Bε) identified in Chinese patients with vanishing white matter disease. J Hum Genet 2011;56:300–5.
[14] Matsukawa T, Wang X, Liu R, Wortham N, Onuki Y, Kubota A, et al. Adult-onset leukoencephalopathies with vanishing white matter with novel missense mutations in EIF2B2, EIF2B3, and EIF2B5. Neurogenetics 2011;12:259–61.
[15] La Piana R, Vanderver A, van der Knaap M, et al. ADult-onset vanishing white matter disease due to a novel eif2b3 mutation. Arch Neurol 2012;69:765–8.
[16] Alsalem A, Shaheen R, Alkuraya FS. Vanishing white matter disease caused by EIF2B2 mutation with the presentation of an adrenoleukodystrophy phenotype. Gene 2012;496:141–3.
[17] van der Knaap MS, Kamphorst W, Barth PG, Kraaijeveld CL, Gut E, Valk J. Phenotypic variation in leukoencephalopathy with vanishing white matter. Neurology 1998;51:540–7.
[18] Yamamoto T, Nanba E, Ninomiya H, Higaki K, Taniguchi M, Zhang H, et al. NPC1 gene mutations in Japanese patients with Niemann–Pick disease type C. Hum Genet 1999;105:10–6.
[19] Shimojima K, Komoike Y, Tohyama J, Takahashi S, Paez MT, Nakagawa E, et al. TULIP1 (RALGAPA1) haploinsufficiency with brain development delay. Genomics 2009;94:414–22.
[20] Kumar P, Henikoff S, Ng PC. Predicting the effects of coding non-synonymous variants on protein function using the SIFT algorithm. Nat Protoc 2009;4:1073–81.
[21] Adzhubei IA, Schmidt S, Peshkin L, Ramensky VE, Gerasimova A, Bork P, et al. A method and server for predicting damaging missense mutations. Nat Methods 2010;7:248–9.
[22] Kircher M, Witten DM, Jain P, O'Roak BJ, Cooper GM, Shendure J. A general framework for estimating the relative pathogenicity of human genetic variants. Nat Genet 2014;46:310–5.
[23] Shimojima K, Narita A, Maegaki Y, Saito A, Furukawa T, Yamamoto T. Whole-exome sequencing identifies a de novo TUBA1A mutation in a patient with sporadic malformations of cortical development: a case report. BMC Res Notes 2014;7:465.
[24] Fogli A, Schiffmann R, Bertini E, Ughetto S, Combes P, Eymard-Pierre E, et al. The effect of genotype on the natural history of eIF2B-related leukodystrophies. Neurology 2004;62:1509–17.
[25] Matsukawa T, Wang X, Liu R, Wortham NC, Onuki Y, Kubota A, et al. Adult-onset leukoencephalopathies with vanishing white matter with novel missense mutations in EIF2B2, EIF2B3, and EIF2B5. Neurogenetics 2011;12:259–61.
[26] Shimada S, Miya K, Oda N, Watanabe Y, Kumada T, Sugawara M, et al. An unmasked mutation of EIF2B2 due to submicroscopic deletion of 14q24.3 in a patient with vanishing white matter disease. Am J Med Genet A 2012;158A:1771–7.
[27] van der Lei HD, Steenweg ME, Barkhof F, de Grauw T, d'Hooghe M, Morton R, et al. Characteristics of early MRI in children and adolescents with vanishing white matter. Neuropediatrics 2012;43:22–6.
[28] Scheper GC, van der Knaap MS, Proud CG. Translation matters: protein synthesis defects in inherited disease. Nat Rev Genet 2007;8:711–23.
[29] Pavitt GD. EIF2B, a mediator of general and gene-specific translational control. Biochem Soc Trans 2005;33:1487–92.
[30] Liu R, van der Lei HD, Wang X, Wortham NC, Tang H, van Berkel CG, et al. Severity of vanishing white matter disease does not correlate with deficits in eIF2B activity or the integrity of eIF2B complexes. Hum Mutat 2011;32:1036–45.
[31] van der Voorn JP, van Kollenburg B, Bertrand G, Van Haren K, Scheper GC, Powers JM, et al. The unfolded protein response in vanishing white matter disease. J Neuropathol Exp Neurol 2005;64:770–5.
[32] Bugiani M, Boor I, Powers JM, Scheper GC, van der Knaap MS. Leukoencephalopathy with vanishing white matter: a review. J Neuropathol Exp Neurol 2010;69:987–96.
[33] Kantor L, Pinchasi D, Mintz M, Hathout Y, Vanderver A, Elroy-Stein O. A point mutation in translation initiation factor 2B leads to a continuous hyper stress state in oligodendroglial-derived cells. PLoS ONE 2008;3:e3783.

Journal of the Neurological Sciences 351 (2015) 211–213

Contents lists available at ScienceDirect

Journal of the Neurological Sciences

journal homepage: www.elsevier.com/locate/jns

Letter to the Editor

Megalencephalic leukoencephalopathy with subcortical cysts caused by compound heterozygous mutations in *MLC1*, in patients with and without subcortical cysts in the brain

Keywords:
Van der Knaap disease
Megalencephalic leukoencephalopathy
Subcortical cysts
MLC1 mutation
MRI
Astrocytes

To the Editor,

Megalencephalic leukoencephalopathy with subcortical cysts (MLC) is a rare hereditary disorder characterized by infantile-onset macrocephaly and a gradual onset of progressive neurological symptoms including ataxia, spasticity, and mild mental decline [1]. As the name of the disorder suggests, patients with MLC invariably had subcortical cysts in the anterior temporal region of the brain [1].

Mutations in two different genes, *MLC1* and *GLIALCAM*, may cause MLC [1,2]. Homozygous or compound heterozygous mutations of *MLC1* were reportedly found in approximately 75% of MLC patients. MLC1 is a plasma membrane protein expressed in the brain and is mainly localized in astrocyte–astrocyte junctions and Bergmann glial cells [3,4]. Although pathophysiological functions of the MLC1 protein remain to be fully elucidated, this protein may be involved in ion transport and water homeostasis [1,5].

In this manuscript, we report on two adult MLC patients who had compound heterozygous mutations, p.Ser93Leu/Ala275Asp, in the *MLC1* gene with and without subcortical cysts in the brain. These findings are important for making an accurate diagnosis of this disease.

1. Case report

A 21-year-old female patient (case 1) was the second child to healthy and non-consanguineous parents. Her birth weight, length, and head circumference were 2988 g (25th–75th percentile), 51 cm (5th–95th percentile), and 34.5 cm (25th–75th percentile), respectively. Her head circumference was 43.5 cm (more than 95th percentile) at 3 months of age, which indicated mild macrocephaly. She rolled over and controlled her head at 4 and 8 months of age, respectively. She walked alone at 16 months of age, but with some difficulty. She showed a gait disturbance at 2.5 years of age and lost the ability to walk and sit unsupported at 3 years of age. Generalized clonic–tonic seizures occurred at 3 years of age and continued until 9 years of age. She was treated with sodium valproate. Brain magnetic resonance imaging (MRI) at 3 years old revealed extensive bilaterally symmetrical white matter changes. She was undiagnosed at that time. Her symptoms progressed gradually. At 21 years of age, she had dysarthria, spasticity, and ataxia. Mental impairment was not observed. Her mini-mental state examination (MMSE) score was 29/30. Brain MRI revealed a diffuse high intensity in the cerebral white matter on fluid-attenuated inversion recovery (FLAIR) images; subcortical cysts were not found in all sections (axial, coronal, sagittal image) in the brain (Fig. 1A-F).

Her younger sister, an 18-year-old female patient (case 2), had been previously diagnosed as having unclassified leukoencephalopathy. Her birth weight, length, and head circumference were 2904 g (25th–75th percentile), 48 cm (25th–75th percentile), and 31 cm (5th–95th percentile), respectively. She rolled over and controlled her head at 5 and 8 months of age, respectively. She walked alone at 18 months of age but fell down easily. She lost the ability to walk and sit unsupported at 2 years of age. At 18 years of age, she also had dysarthria, spasticity, and ataxia without mental impairment. Her MMSE score was 28/30. Brain MRI FLAIR images revealed a diffuse high intensity in the cerebral white matter, with subcortical cysts in the bilateral anterior temporal region (Fig. 1G-J).

We analyzed the *MLC1* cDNA from peripheral leukocytes by using sequence analysis [6] in case 1, case 2, and their parents after we had obtained informed consent. Case 1 and case 2 had compound heterozygous mutations, c. 393C > T (p.Ser93Leu) in exon 4 and c. 823C > A (p.Ala275Asp) in exon 10. Their father had a heterozygous p.Ala275Asp mutation, and their mother had a heterozygous p.Ser93Leu mutation. On the basis of these genetic analysis results, we diagnosed the sisters as having MLC.

2. Discussion

Here, we described two Japanese sisters affected with MLC that was caused by compound heterozygous mutations, p.Ser93Leu/Ala275Asp, in the *MLC1* gene. *MLC1* p.Ser93Leu and p.Ala275Asp mutations were frequently found, especially in Japanese MLC patients [6–9]. Although these two sisters with MLC caused by the same compound heterozygous mutations had similar clinical disease courses and symptoms, subcortical cysts occurred in the brain of only one patient (case 2).

As the name of the disorder suggests, the presence of subcortical cysts in the anterior temporal region, and frequently also in the frontal and parietal regions, is a hallmark of MLC [1]. We did not find any cysts, however, in one MLC patient (case 1). To the best of our knowledge, this patient (case 1) is the first MLC case without subcortical cysts findings in MRI. This patient (case 1) with leukoencephalopathy did not receive a definitive diagnosis until she was 21 years old because

Abbreviations: MLC, megalencephalic leukoencephalopathy with subcortical cysts; MRI, magnetic resonance imaging; FLAIR, fluid-attenuated inversion recovery.

http://dx.doi.org/10.1016/j.jns.2015.03.010

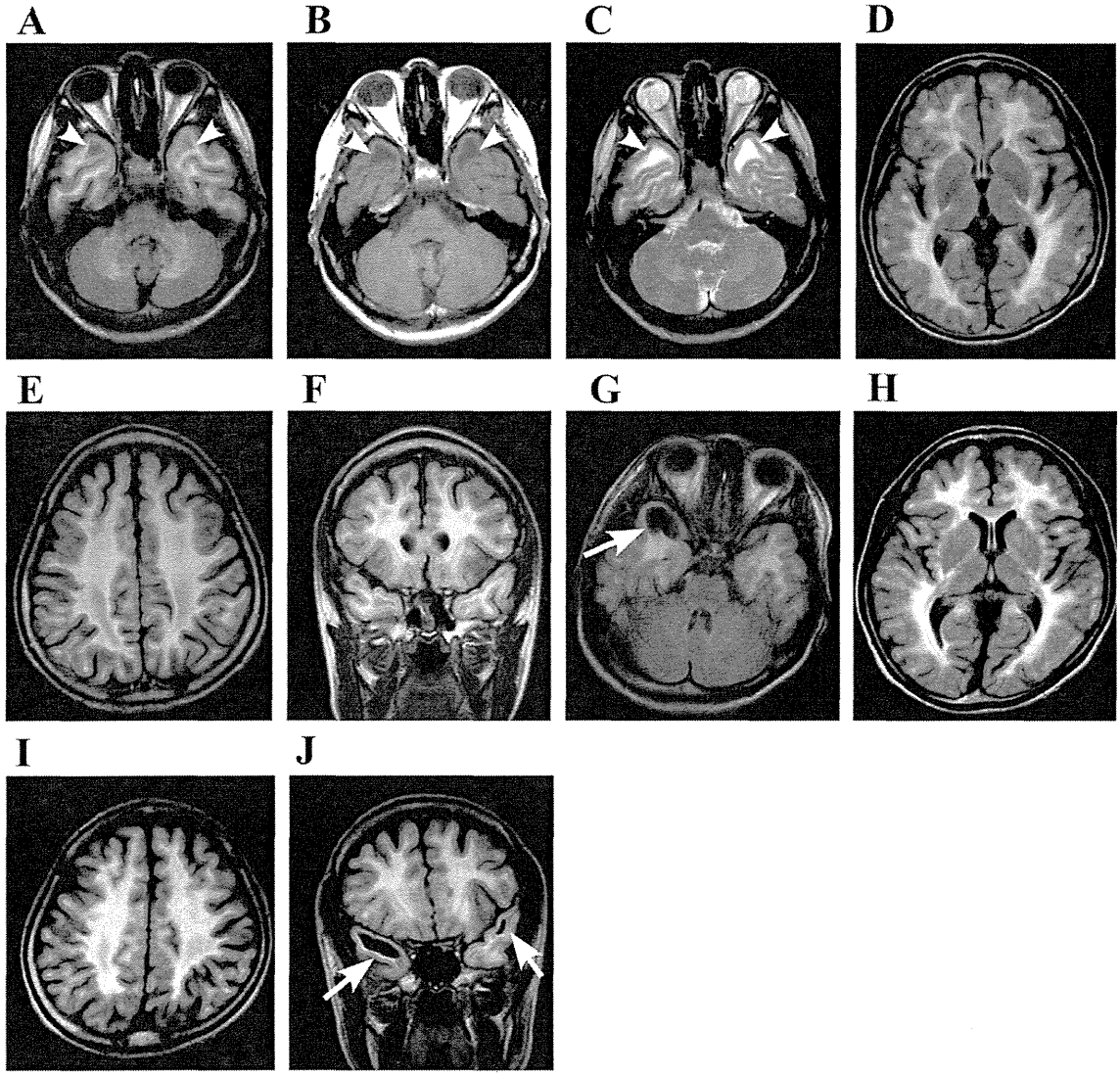

Fig. 1. Brain MRI images of the two adult sisters with MLC. (A–F) Case 1 (II-2). (G–J) Case 2 (II-3). (A, D–J) FLAIR images. (B) T1-weighted image. (C) T2-weighted image. Arrows point to subcortical cysts in the anterior temporal region; the arrowheads indicate anterior temporal lesions without cystic changes in MRI.

her brain MRI did not show the typical subcortical cyst findings. MRI findings in her younger sister (case 2) provided an important clue to her definitive diagnosis. As clinicians attempting to make an accurate diagnosis of MLC, we should understand that certain MLC patients may not have subcortical cysts in the brain.

Via careful evaluation of the FLAIR images, we found small lesions which were isointense with the cortex in the white matter of the anterior temporal region in case 1 (Fig. 1C). These lesions were low intensity in T1-weighted image and high intensity in T2-weighted image. Van der Knaap et al. reported that MLC patients had large numbers of microscopic vacuoles in the white matter based on histopathological examinations [10]. The anterior temporal lesions which were isointense with the cortex without cysts in the FLAIR images may have microscopic vacuoles in the white matter. Since subcortical cysts in MLC might change in size and number over time, subcortical cysts could have been present on earlier MRIs in the case 1. Also, longitudinal follow-up evaluation of this MRI finding should be performed.

In conclusion, in this report, we described two adult sisters with MLC caused by compound heterozygous mutations of *MLC1*, one sister with and one sister without subcortical cysts in the brain. We should thus include MLC in the differential diagnosis of leukoencephalopathy, even in adult patients without subcortical cysts.

Declaration of conflict of interest

The authors declare no conflicts of interest.

Acknowledgments

We would like to thank all members of Department of Neurology, Kumamoto Saisyunsou National Hospital, for helping with the collection of clinical data. We are indebted to Ms. Judith B. Gandy for providing professional English editing of the manuscript.

References

[1] van der Knaap MS, Boor I, Estévez R. Megalencephalic leukoencephalopathy with subcortical cysts: chronic white matter oedema due to a defect in brain ion and water homoeostasis. Lancet Neurol 2012;11:973–85.
[2] López-Hernández T, Ridder MC, Montolio M, Capdevila-Nortes X, Polder E, Sirisi S, et al. Mutant GlialCAM causes megalencephalic leukoencephalopathy with subcortical cysts, benign familial macrocephaly, and macrocephaly with retardation and autism. Am J Hum Genet 2011;88:422–32.
[3] Boor PK, de Groot K, Waisfisz Q, Kamphorst W, Oudejans CB, Powers JM, et al. MLC1: a novel protein in distal astroglial processes. J Neuropathol Exp Neurol 2005;64:412–9.
[4] Teijido O, Martínez A, Pusch M, Zorzano A, Soriano E, Del Río JA, et al. Localization and functional analyses of the MLC1 protein involved in megalencephalic leukoencephalopathy with subcortical cysts. Hum Mol Genet 2004;13:2581–94.

[5] Schmitt A, Gofferje V, Weber M, Meyer J, Mössner R, Lesch KP. The brain-specific protein MLC1 implicated in megalencephalic leukoencephalopathy with subcortical cysts is expressed in glial cells in the murine brain. Glia 2003;44:283–95.
[6] Shimada S, Shimojima K, Masuda T, Nakayama Y, Kohji T, Tsukamoto H, et al. *MLC1* mutations in Japanese patients with megalencephalic leukoencephalopathy with subcortical cysts. Hum Genome Var 2014;1:14019.
[7] Montagna G, Teijido O, Eymard-Pierre E, Muraki K, Cohen B, Loizzo A, et al. Vacuolating megalencephalic leukoencephalopathy with subcortical cysts: functional studies of novel variants in *MLC1*. Hum Mutat 2006;27:292.
[8] Itoh N, Maeda M, Naito Y, Narita Y, Kuzuhara S. An adult case of megalencephalic leukoencephalopathy with subcortical cysts with S93L mutation in MLC1 gene: a case report and diffusion MRI. Eur Neurol 2006;56:243–5.
[9] Koyama S, Kawanami T, Arawaka S, Wada M, Kato T. A Japanese adult case of megalencephalic leukoencephalopathy with subcortical cysts with a good long-term prognosis. Intern Med 2012;51:503–6.
[10] van der Knaap MS, Barth PG, Vrensen GF, Valk J. Histopathology of an infantile-onset spongiform leukoencephalopathy with a discrepantly mild clinical course. Acta Neuropathol 1996;92:206–12.

Teruaki Masuda
Department of Neurology, National Hospital Organization, Kumamoto Saisyunsou Hospital, 2659 Suya, Koshi City, Kumamoto 861-1196, Japan
Department of Neurology, Graduate School of Medical Sciences, Kumamoto University, 1-1-1 Honjo, Chuo-ku, Kumamoto 860-8556, Japan

Mitsuharu Ueda
Department of Neurology, Graduate School of Medical Sciences, Kumamoto University, 1-1-1 Honjo, Chuo-ku, Kumamoto 860-8556, Japan
Corresponding author. Tel.: +81 96 373 5893; fax: +81 96 373 5895.
E-mail address: mitt@rb3.so-net.ne.jp.

Hidetsugu Ueyama
Department of Neurology, National Hospital Organization, Kumamoto Saisyunsou Hospital, 2659 Suya, Koshi City, Kumamoto 861-1196, Japan

Shino Shimada
Tokyo Women's Medical University Institute for Integrated Medical Sciences, 8-1 Kawata-cho, Shinjuku-ku, Tokyo, 162-8666, Japan

Masatoshi Ishizaki
Department of Neurology, National Hospital Organization, Kumamoto Saisyunsou Hospital, 2659 Suya, Koshi City, Kumamoto 861-1196, Japan

Shigehiro Imamura
Department of Neurology, National Hospital Organization, Kumamoto Saisyunsou Hospital, 2659 Suya, Koshi City, Kumamoto 861-1196, Japan

Toshiyuki Yamamoto
Tokyo Women's Medical University Institute for Integrated Medical Sciences, 8-1 Kawata-cho, Shinjuku-ku, Tokyo, 162-8666, Japan

Yukio Ando
Department of Neurology, Graduate School of Medical Sciences, Kumamoto University, 1-1-1 Honjo, Chuo-ku, Kumamoto 860-8556, Japan

30 January 2015

Neurology® Clinical Practice

Cases

Characteristic abnormal signals in medulla oblongata—"eye spot" sign

Four cases of elderly-onset Alexander disease

Tomokatsu Yoshida, MD, PhD
Ikuko Mizuta, MD, PhD
Kozo Saito, MD
Yasuyoshi Kimura, MD
Kwiyoung Park, MD
Yasuo Ito, MD, PhD
Shotaro Haji, MD
Masanori Nakagawa, MD, PhD
Toshiki Mizuno, MD, PhD

Alexander disease (AxD) is a rare neurodegenerative disorder with a prevalence rate of 1 in 2,700,000.[1] Its pathologic characteristics include the formation of cytoplasmic inclusions in astrocytes, called Rosenthal fibers, and white matter degeneration.[2] The genetic mutation of glial fibrillary acidic protein (*GFAP*)[3] is observed in approximately 97% of cases.

In type 2 AxD,[1] which is usually adult-onset, marked atrophy and abnormal signals in the medulla oblongata and cervical cord are characteristic MRI findings.[3–5] When the bulge of the basilar part of the pons remains and atrophy of the medulla oblongata and cervical cord is marked,[6] AxD is strongly suspected.

However, there is no clear standard by which to assess atrophy of the medulla oblongata, and it has been speculated that it becomes more difficult to suspect AxD when the degree of atrophy is mild to moderate. We report 4 AxD patients with an onset age older than 50 years in whom characteristic abnormality of the signal intensity of the anterior portion of the medulla oblongata along with mild to moderate atrophy of the medulla oblongata were observed.

The cases represent 4 patients who were suspected to have AxD and referred to Kyoto Prefectural University of Medicine for *GFAP* gene analysis.

Practical Implications

Bilateral abnormal signals of the anterior portion of the medulla oblongata on MRI may be helpful in diagnosing Alexander disease.

Department of Neurology (TY, IM, KS, TM), Graduate School of Medical Science, and Department of Neurology (MN), North Medical Center, Kyoto Prefectural University of Medicine; Department of Neurology (YK), Osaka University Graduate School of Medicine; Department of Neurology (KP), National Hospital of Utano, Kyoto; Department of Neurology (YI), Faculty of Medicine, Saitama Medical University; and Department of Neurology (SH), Hiroshima City Asa Hospital, Japan.

Funding information and disclosures are provided at the end of the article. Full disclosure form information provided by the authors is available with the **full text of this article at Neurology.org/cp**.

Correspondence to: toyoshid@koto.kpu-m.ac.jp

Figure Brain MRI of the 4 patients

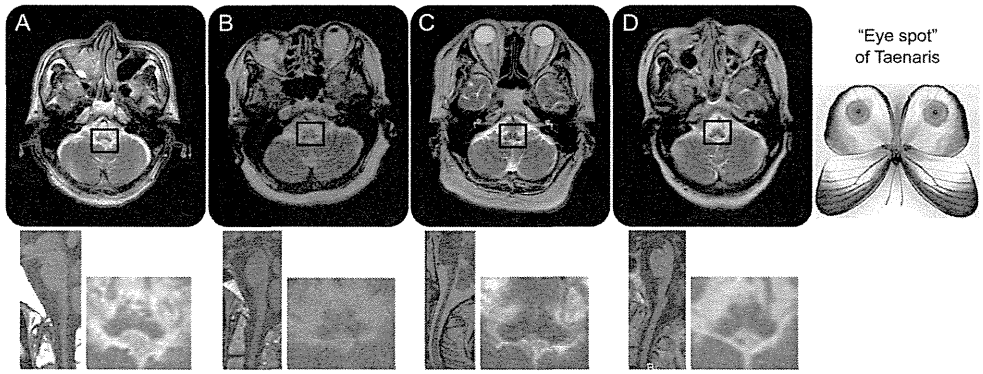

The upper, lower right, and lower left sections of each case show an axial image of the pyramids, an extended image of the medulla oblongata, and a sagittal image, respectively. Symmetrical signal abnormality of anterior and lateral portions was observed in all cases. It resembles the "eye spot" of *Taenaris* in the medulla oblongata with mild to moderate atrophy. The figure of *Taenaris diana* was cited from http://www.pteron-world.com.

Case A

Fatigability during walking developed when the patient was 62 years old, gait disturbance was noted and deteriorated at the age of 64, and subsequently speech disturbance and difficulty swallowing appeared. The patient was hospitalized at age 65 with dysarthria, dysphagia, nystagmus, muscle weakness of the extremities (especially the left upper extremity), increased tendon reflexes of the lower extremities, bilateral Babinski sign, mild trunk and limb ataxia, an ataxic and spastic gait, sphincter abnormalities, and obstructive sleep apnea.

Case B

Impending incontinence and dropped head syndrome appeared at the age of 58 years, and trunk ataxia was noted at age 60. Central sleep apnea was observed at the age of 62. Increased tendon reflexes of the right upper extremity, bilateral Babinski sign, dysphagia, trunk and limb ataxia, orthostatic hypotension, sphincter abnormalities, and scoliosis were noted at age 65.

Case C

After undergoing lumbar laminectomy for paraparesis at the age of 60 years, muscle weakness of the bilateral upper extremities and dysarthria appeared. Muscle weakness of the extremities, increased tendon reflexes of the upper extremities, bilateral Babinski sign, dysarthria, dysphonia, and sleep apnea were observed at age 65.

Case D

Dysarthria and spastic gait had gradually progressed from the age of 64. She was hospitalized at age 65, showing tendon reflexes, bilateral Babinski sign, dysarthria, dysphagia, and limb and trunk ataxia.

MRI findings for each case are presented in the figure and the table, and abnormal signals in the anterior and lateral portions of the medulla oblongata were observed in all patients. Abnormal signals in the hilum of the dentate nucleus and periventricular abnormality were noted in cases B and D. Inferior olivary hypertrophy was not detected on MRI.

DISCUSSION

The following have been reported as characteristic MRI findings in patients with type II AxD: (1) progressive atrophy of the medulla oblongata and upper spinal cord with or without hyperintensities on T2-weighted images,[1,4,5] (2) involvement of the hilum of the dentate nucleus,[1,4,5] (3) supratentorial periventricular abnormalities in signal intensity and spotty areas of postcontrast enhancement,[4] and (4) pial fluid-attenuated inversion recovery signal

Table Summary of clinical features and MRI findings of the 4 patients

Patient	A	B	C	D
GFAP mutation	N386S	E210K	R258H	R70W
Sex	M	F	M	F
Age at onset, y	62	58	60	64
Age at diagnosis, y	65	65	65	65
Neurologic symptoms				
Weakness	+	−	+	−
Spasticity/hyperreflexia	+	+	+	+
Dysarthria	+	−	+	+
Dysphagia	+	+	+	+
Nystagmus	+	+	+	−
Ataxia	+	+	+	+
Palatal tremor	−	−	−	−
Autonomic dysfunction	+	+	−	−
Sleep disorder	+	+	+	−
MRI findings				
Atrophy of medulla oblongata	Moderate	Mild	Moderate	Mild
Abnormal signal of frontal and lateral portions of medulla oblongata	+	+	+	+
Involvement of the hilum of the dentate nucleus	−	+	−	+
Periventricular abnormalities	−	+	−	+

abnormality and middle peduncle signal change or enhancement.[5] The frequency of signal abnormality of the medulla oblongata varies with the age at onset, and it is observed in various subregions, especially in juvenile-onset patients. In the present 4 patients with elderly-onset AxD and mild to moderate atrophy of the medulla oblongata, the low intensity of the lateral portion of the medulla oblongata has the configuration of butterfly wings, and the signal abnormality in the anterior portion of the medulla oblongata resembles the "eye spot" of *Taenaris*. The signal abnormality of the anterior portion on MRI may reflect myelin loss of the bilateral pyramids.[7] As degeneration of the medulla oblongata progresses, the "eye spot" sign disappears and the frontal portion of the medulla oblongata becomes atrophic, which may reflect cavity change of the pyramids.[7]

Elderly-onset AxD tends to be more indolent, and the degree of atrophy of the medulla oblongata tends to be milder compared to the early-adult–onset form, which develops in the 20s–40s. The characteristic signal abnormality of the anterior portion of the medulla oblongata that we reported, for which we propose the term "eye spot" sign, is considered to be a useful finding indicating AxD in elderly-onset cases.

REFERENCES

1. Yoshida T, Sasaki M, Yoshida M, et al. Nationwide survey of Alexander disease in Japan and proposed new guidelines for diagnosis. J Neurol 2011;258:1998–2008.
2. Alexander WS. Progressive fibrinoid degeneration of fibrillary astrocytes associated with mental retardation in a hydrocephalic infant. Brain 1949;72:373–381.
3. Brenner M, Johnson AB, Boespflug-Tanguy O, Rodriguez D, Goldman JE, Messing A. Mutations in GFAP, encoding glial fibrillary acidic protein, are associated with Alexander disease. Nat Genet 2001; 27:117–120.

4. Farina L, Pareyson D, Minati L, et al. Can MR imaging diagnose adult-onset Alexander disease? AJNR Am J Neuroradiol 2008;29:1190–1196.
5. Graff-Radford J, Schwartz K, Gavrilova RH, Lachance DH, Kumar N. Neuroimaging and clinical features in type II (late-onset) Alexander disease. Neurology 2014;82:49–56.
6. Namekawa M, Takiyama Y, Honda J, Shimazaki H, Sakoe K, Nakano I. Adult-onset Alexander disease with typical "tadpole" brainstem atrophy and unusual bilateral basal ganglia involvement: a case report and review of the literature. BMC Neurol 2010;10:21.
7. Namekawa M, Takiyama Y, Aoki Y, et al. Identification of GFAP gene mutation in hereditary adult-onset Alexander's disease. Ann Neurol 2002;52:779–785.

STUDY FUNDING

No targeted funding reported.

DISCLOSURES

T. Yoshida receives funding from a Grant-in-Aid for Scientific Research (C) from Japan Society for the Promotion of Science (grant number 24591273) and from a Grant-in-Aid for Challenging Exploratory Research (grant number 24659433). I. Mizuta receives funding from a Grant-in-Aid for Scientific Research (C) from Japan Society for the Promotion of Science (grant number 24591273). K. Saito, Y. Kimura, K. Park, Y. Ito, and S. Haji report no disclosures. M. Nakagawa has received research support from the Intractable Disease Research Grants, from the Ministry of Health, Labour, and Welfare of the Government of Japan, and from a Grant-in-Aid for Challenging Exploratory Research (grant number 24659433). T. Mizuno reports no disclosures. Full disclosure form information provided by the authors is available with the **full text of this article at Neurology.org/cp**.

Journal of the Neurological Sciences 354 (2015) 131–132

Contents lists available at ScienceDirect

Journal of the Neurological Sciences

journal homepage: www.elsevier.com/locate/jns

Letter to the Editor

Incidental diagnosis of an asymptomatic adult-onset Alexander disease by brain magnetic resonance imaging for preoperative evaluation

Keywords:
Incidental diagnosis
Alexander disease
GFAP
Asymptomatic
Genetic testing

1. Introduction

Alexander disease (AD) is pathologically characterized by accumulation of Rosenthal fibers, which comprise glial fibrillary acidic protein (GFAP) and αB-crystalline and heat shock protein 27 in the cytoplasm of perivascular and subpial astrocyte end feet. Based on age of onset, three forms of AD, caused by *GFAP* mutation, are recognized: infantile, juvenile, and adult [1,2]. Following *GFAP* identification and diagnostic magnetic resonance imaging (MRI), cases of adult-onset AD (AOAD) are being described with increasing frequency. Although recent reports have shown that AOAD has a wide clinical variability [3], asymptomatic cases incidentally diagnosed by MRI have been rarely reported.

1.1. Case report

A 72-year-old man, with no neurological complaints, was referred to our department because of brain MRI abnormalities. He had no family history of AD, but his mother had been diagnosed with Parkinson's disease and died at age 64. He was a 400-meter hurdler in his college days. His past medical history included hypertension, cardiac angina, and transient diplopia interpreted as a manifestation of a transient ischemia of the brainstem. At age 72, he was diagnosed with prostate cancer, and a brain MRI was performed for preoperative evaluation because of past stroke history.

Dysarthria, dysphasia, and palatal myoclonus were not observed. Left side deep tendon reflexes were mildly increased, but plantar responses were flexor, and there were no signs of spasticity. No muscle fasciculation or weakness or sensory abnormality was observed. His gait was normal, and he could stand with Mann's position, but was unable to perform tandem gait walking. Brain MRI showed atrophy of the upper cervical cord, medulla oblongata, and cerebellum (Fig. 1).

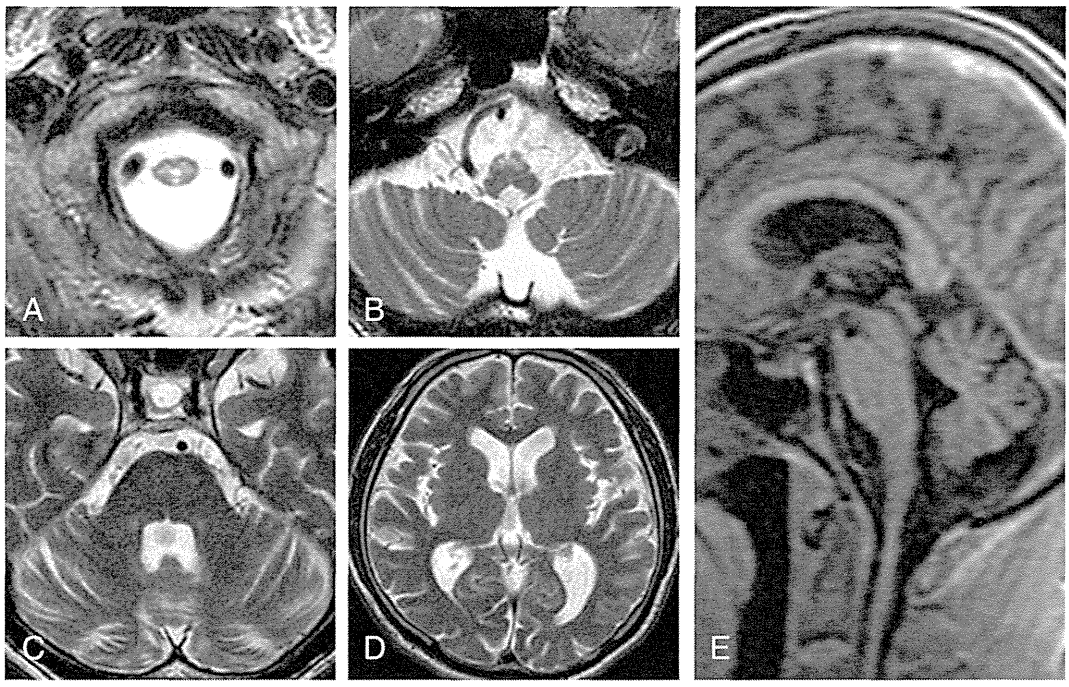

Fig. 1. A and B, axial T2-weighted images show atrophy of the upper cervical cord and medulla oblongata. There are bilateral abnormal hyperintensities in the ventral medulla oblongata. C, There are abnormal bilateral hyper-intensities in the dentate nuclei, and cerebellar atrophy. D, There are no apparent white matter lesions. E, An image of the scout view suggests atrophy of the medulla oblongata and upper cervical cord.

http://dx.doi.org/10.1016/j.jns.2015.05.001

There were bilateral T2-hyperintensity lesions in the ventral medulla oblongata and hilum of the dentate nuclei. There were subtle and non-specific cerebral white matter changes. Although there were only minimal signs from neurological examination, such MRI abnormalities led us to consider a diagnosis of AD and prompted genetic testing. Sequence analysis of the *GFAP* with informed consent revealed a heterozygous c.1157A > G mutation, predicting a p.N386S amino acid change.

2. Discussion

Here we describe an asymptomatic AOAD case. His diagnosis was led by brain MRI performed for preoperative evaluation of prostate cancer and confirmed genetically. The patient's past history of diplopia raised concerns about the possible symptoms of AD because there was no apparent vascular abnormality in the brainstem on MRI that could cause diplopia. In contrast, diplopia is an atypical first symptom of AOAD, and its sudden onset and transient course suggest an occurrence of stroke. It is much more likely that a minor stroke, invisible on MRI, caused the patient's diplopia. His mother had been diagnosed with Parkinson's disease, and details of her clinical course were unknown. There was a little possibility that her extrapyramidal symptoms were caused by undiagnosed AD.

Although diagnostic MRI criteria for infantile AD have been defined by van der van der Knaap et al. [4], recent studies suggest that the radiologic presentation of AOAD significantly differs from infantile-onset cases [5,6]. AOAD cases appear to have less cerebral white matter involvement. The severe atrophy of the medulla oblongata and spinal cord, and signal abnormalities in the hilum of the dentate nucleus are frequently presented in AO cases. Brain MRI of this patient revealed a marked atrophy of the upper cervical cord, medulla oblongata, and cerebellum as well as bilateral T2-hyperintense lesions in the ventral medulla oblongata and in the hilum of the dentate nuclei. These findings correlate well with the abnormalities reported as characteristic findings of AOAD and led us to consider genetic testing for the *GFAP* mutation.

Although several reports have already described asymptomatic AD cases, most of them had an apparent family history and were young or middle-aged people [3,5,7]. The patient in this case is not only an asymptomatic AOAD case with characteristic MRI findings but has no apparent family history and is the oldest of the previously reported asymptomatic patients.

Before identification of the *GFAP* mutation in AD, some neurologically asymptomatic adult cases with heavy deposits of Rosenthal fibers in the central nervous system have been identified in autopsy [8]. There may be some phenotypes showing typical MRI abnormalities, reflecting pathological deposits of Rosenthal fibers, and present no or only subtle neurological symptoms. In these phenotypes, family history is usually unrecognized and patients are likely underdiagnosed. The reason for discrepancies between marked MR abnormalities and scarce neurological impairment is unknown. In cases of AD with clinical course of acute exacerbation and remission, acute exacerbation was caused by fall down, fever, and excessive alcohol consumption [9,10]. In addition to deposition of Rosenthal fibers, other factors may be associated with presentation of neurological symptoms.

AOAD diagnosis may be proposed even in patients without symptoms and apparent family history. In such cases, characteristic MRI findings are key for proceeding with genetic testing for *GFAP*. When revealed, prompt genetic counseling is recommended.

Conflict of interest

The authors declare no conflict of interest.

References

[1] Brenner M, Johnson AB, Boespflug-Tanguy O, Rodriguez JE, Goldman JE, Messing A. Mutations in GFAP, encoding glial fibrillary acidic protein, are associated with Alexander disease. Nat Genet 2001;27:117–20.

[2] Stumpf E, Masson H, Duquette A, et al. Adult Alexander disease with autosomal dominant transmission: a distinct entity caused by mutation in the glial fibrillary acid protein gene. Arch Neurol 2003;60:1307–12.

[3] Pareyson D, Fancellu R, Mariotti C, et al. Adult-onset Alexander disease: a series of eleven unrelated cases with review of the literature. Brain 2008;131:2321–31.

[4] van der Knaap MS, Naidu S, Breiter SN, et al. Alexander disease: diagnosis with MR imaging. Am J Neuroradiol 2001;22:541–52.

[5] Farina L, Pareyson D, Minati L, et al. Can MR imaging diagnose adult-onset Alexander disease? AJNR Am J Neuroradiol 2008;29:1190–6.

[6] Graff-Radford J, Schwartz K, Gavrilova RH, Lachance DH, Kumar N. Neuroimaging and clinical features in type II (late-onset) Alexander disease. Neurology 2014;82:49–56.

[7] Yoshida T, Sasayama H, Mizuta I, et al. Glial fibrillary acidic protein mutations in adult-onset Alexander disease: clinical features observed in 12 Japanese patients. Acta Neurol Scand 2011;124:104–8.

[8] Riggs JE, Schochet SS, Nelson J. Asymptomatic adult Alexander's disease: entity or nosological misconception? Neurology 1988;38:152–4.

[9] Ayaki T, Shinohara M, Tatsumi S, Namekawa M, Yamamoto T. A case of sporadic adult Alexander disease presenting with acute onset, remission and relapse. J Neurol Neurosurg Psychiatry 2010;81:1292–3.

[10] Schmidt H, Kretzschmar B, Lingor P, et al. Acute onset of adult Alexander disease. J Neurol Sci 2013;331:152–4.

Atsuhiko Sugiyama
Department of Neurology, Graduate School of Medicine, Chiba University, Chiba, Japan
Corresponding author at: Department of Neurology, Graduate School of Medicine, Chiba University, 1-8-1 Inohana, Chuo-ku, Chiba 260-8670, Japan. Tel.: +81 43 226 2129; fax: +81 43 226 2160.
E-mail address: chinneosyo0624@yahoo.co.jp.

Setsu Sawai
Department of Neurology, Graduate School of Medicine, Chiba University, Chiba, Japan

Shoichi Ito
Department of Neurology, Graduate School of Medicine, Chiba University, Chiba, Japan
Office of Medical Education, Graduate School of Medicine, Chiba University, Chiba, Japan

Hiroki Mukai
Department of Radiology, Graduate School of Medicine, Chiba University, Chiba, Japan

Minako Beppu
Department of Neurology, Graduate School of Medicine, Chiba University, Chiba, Japan

Tomokatsu Yoshida
Department of Neurology, Graduate School of Medical Science, Kyoto Prefectural University of Medicine, Japan

Satoshi Kuwabara
Department of Neurology, Graduate School of Medicine, Chiba University, Chiba, Japan

18 February 2015

ISSN 0722-5091

DOI 10.5414/NP300806
e-pub: April 1, 2015

An autopsied case of adult-onset bulbospinal-form Alexander disease with a novel S393R mutation in the *GFAP* gene

Yasushi Iwasaki[1] Yufuko Saito[2], Keiko Mori[3] Masumi Ito[3] Maya Mimuro[1], Ikuko Aiba[2] Kozo Saito[4] Ikuko Mizuta[4] Tomokatsu Yoshida[4] Masanori Nakagawa[5] and Mari Yoshida[1]

[1]Department of Neuropathology, Institute for Medical Science of Aging, Aichi Medical University, [2]Department of Neurology, National Hospital Organization Higashi Nagoya National Hospital, Nagoya, [3]Department of Neurology, Oyamada Memorial Spa Hospital, Yokkaichi, [4]Department of Neurology, Graduate School of Medical Science, and [5]Division of Neurology, North Medical Center, Kyoto Prefectural University of Medicine, Kyoto, Japan

Key words
Alexander disease – Rosenthal fiber – S393R – GFAP – astrocyte

Abstract. A 50-year-old Japanese man with no apparent family history noticed diplopia. He gradually showed gait disturbance and dysuria. Abducens disorder of eye movement with nystagmus, tongue atrophy with fasciculation, spastic tetraparesis, and sensory disturbance were also observed. MRI showed severe atrophy of the medulla oblongata to the cervical cord ("tadpole appearance"). Tracheotomy and gastrostomy were performed 7 years after onset due to the development of bulbar palsy. Death occurred following respiratory failure after 11 years total disease duration. The brain weighed 1,380 g. The cerebrum, cerebellum, midbrain, and upper pons were preserved from atrophy, but the medulla oblongata to the cervical cord showed severe atrophy. A few Rosenthal fibers were observed in the cerebral white matter, basal ganglia, and cerebellum, whereas numerous Rosenthal fibers were observed in the medulla oblongata to the cervical cord. Myelin loss with relatively preserved axons was extensively observed from the middle of the pons to the spinal cord. The clinicopathological diagnosis was adult-onset bulbospinal-form Alexander disease. Glial fibrillary acidic protein (*GFAP*) gene analysis revealed a novel mutation of S393R. Expression patterns of S393R mutant GFAP using adrenal carcinoma-derived cells (SW13 cells) showed a decreased number of filamentous structures and abnormal aggregates.

Received
July 23, 2014;
accepted in revised form
January 2, 2015

Correspondence to
Yasushi Iwasaki, PhD
Department of Neuropathology, Institute for Medical Science of Aging, Aichi Medical University, 1-1 Yazako-karimata, Nagakute 480-1195, Japan
iwasaki@sc4.so-net.ne.jp

Introduction

Alexander disease is a rare neurodegenerative and demyelinating disorder that is classified as infantile-type, juvenile-type, or adult-type according to age at disease onset (< 2 years old, 2 – 12 years old, > 12 years old, respectively) [1, 2, 3]. Infantile-type cases show megalencephaly, seizure, loss or delay of developmental milestones, mental deficiency, and spastic tetraparesis, which lead to death within a few years [1, 2, 3]. Juvenile-type cases show mild cognitive impairment, bulbar involvement, muscle weakness, ataxia, hyperreflexia, and variable survival [1, 2, 3]. Adult-type cases are rare, with slow progression of the clinical course that may be reminiscent of Parkinson's disease or multiple sclerosis [1, 2], and in some cases, palatal myoclonus is emphasized [3, 4]. The pathological characteristic is the presence of numerous Rosenthal fibers, which are intracytoplasmic astrocytic inclusions, particularly in the cytoplasm of the perivascular and subpial astrocyte end-feet [1, 2]. Recently, new guidelines for the classification of Alexander disease into three distinct clinical types on the basis of neurological and MRI findings were proposed: cerebral form (type 1), in which onset occurs primarily in infancy with abnormalities in the frontal cerebral white matter observed on MRI, bulbospinal form (type 2), in which onset occurs primarily in adulthood with atrophy and signal abnormalities of the medulla oblongata to the upper cervical cord observed on MRI, and intermediate form (type 3), which has the characteristics of both forms and of long-term survivors with cerebral form [1, 4]. This classification gives further understanding of Alexander disease, but a need exists for fur-

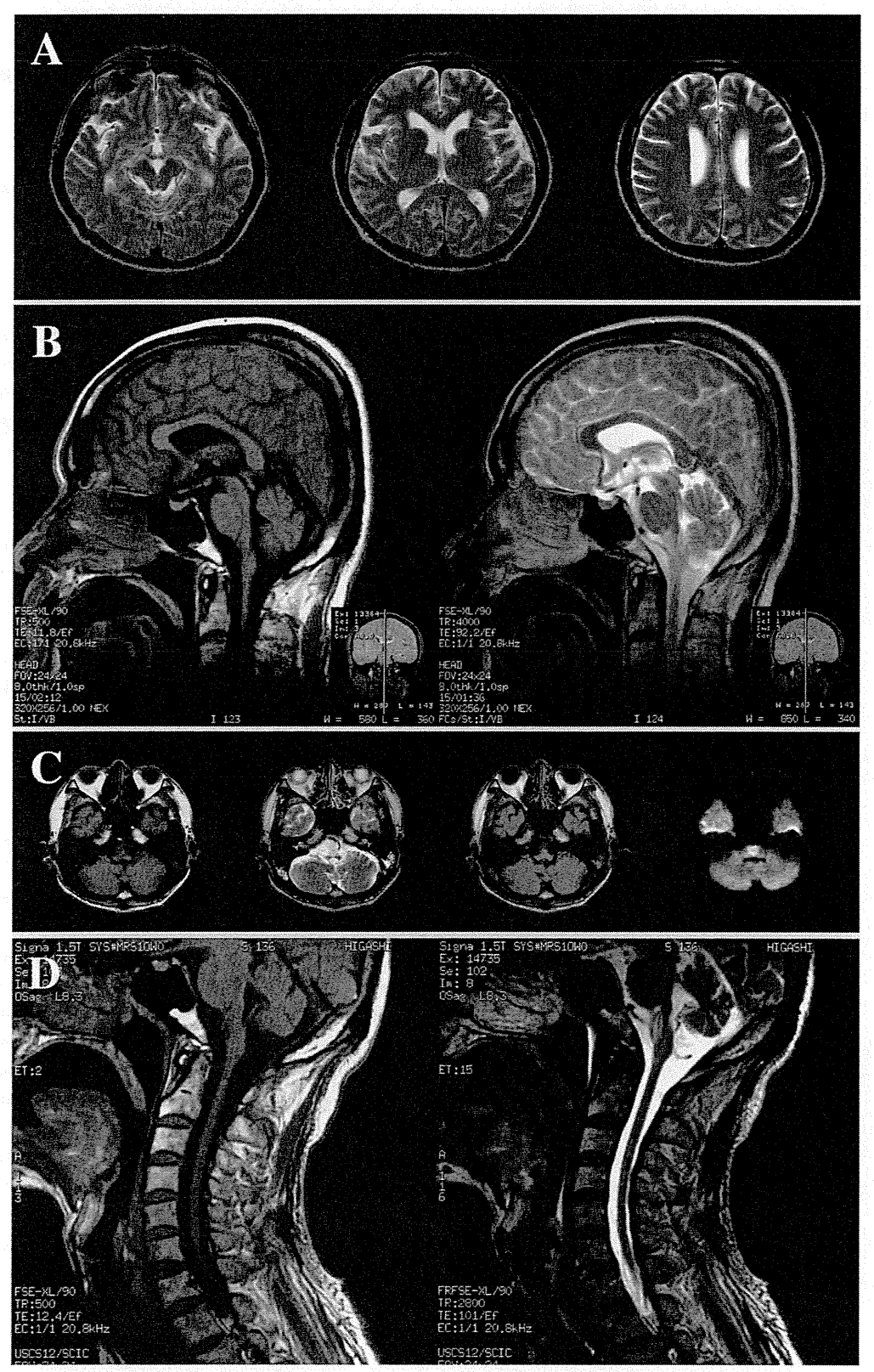

Figure 1 Head MRI obtained 6 years after onset. A: Axial T_2-weighted images of the brain. Although mild dilatation of the anterior horn is observed, no apparent cerebral atrophy or white matter degeneration is recognized (left: at the level of midbrain, middle: at the level of basal ganglia, and right: at the level of corona radiata). B: Midline sagittal images of the brain. Severe atrophy with changes in signal intensity from the medulla oblongata to the upper cervical cord ("tadpole appearance") is observed (left: T_1-weighted image, right: T_2-weighted image). C: Axial images at the level of the lower brainstem show severe atrophy of the medulla oblongata. Diffusion-weighted image shows hyperintensity of the medulla oblongata (left to right: T_1-weighted image, T_2-weighted image, fluid-attenuated inversion recovery image, and diffusion-weighted image). D: Midline sagittal image of the cervical cord. Diffuse atrophy is observed from the medulla oblongata to the cervical cord (left: T_1-weighted image, right: T_2-weighted image).

ther genetic and clinicopathologic investigation.

We report on the clinicopathologic, genetic, and experimental investigations of an autopsied case of adult-onset bulbospinal-form Alexander disease with a novel S393R mutation in the glial fibrillary acidic protein (*GFAP*) gene.

Case report

The patient was a Japanese man living in Aichi prefecture, Japan. He noticed diplopia at the age of 50. He had no remarkable past history and was not under treatment for any disease. There was no family history of similar symptoms or neurodegenerative disorders, and his parents were not consanguineous. Six months after the onset of symptoms, an operation was performed for strabismus and the patient's diplopia temporarily improved, but eventually recurred. The following year, he noticed dysuria and was diagnosed with neurogenic bladder. At 3 years after onset, the patient gradually began to notice gait disturbance, and muscle weakness of his extremities progressed. At 5 years after onset, he could not continue his job and was admitted to the Department of Neurology. Neurological examination revealed an abducens disorder of eye movement with nystagmus, spastic tetraparesis, and sensory disturbance. Tongue atrophy with fasciculation was observed, but palatal myoclonus was not apparent. The deep tendon reflexes of his extremities were exaggerated, and bilateral ankle clonus and Babinski sign were present. Orthostatic hypotension was recognized, but there were no episodes of syncope. Head MRI showed severe atrophy with changes in signal intensity from the medulla oblongata to the cervical cord, whereas no abnormalities were found in the cerebrum and cerebellum (Figure 1). Cerebrospinal fluid showed 58 mg/dL glucose, 58 mg/dL protein, 1 lymphocyte/mm^3, and negative oligoclonal IgG band. Electroencephalography showed normal α-wave activity. The electromyogram showed no active denervation potential or fibrillation potential in the limbs. There was no evidence of dementia: the patient's score on the revised version of the Hasegawa dementia scale (a commonly used method in Japan to assess dementia that uses a scale of 0 – 30, where < 21 suggests dementia) was 30. Based on the clinical and MRI findings, adult-onset Alexander disease was suspected. Gene analysis of the patient's DNA, performed by direct sequencing of the whole *GFAP* gene coding region and the adjacent splice sites, showed a novel mutation of S393R (AGC>AGG). Muscle weakness of the patient's extremities gradually progressed with atrophy until he reached a state of complete tetraplegia with extended limb position and joint contracture. Tracheotomy and gastrostomy were performed 7 years after the onset of symptoms due to the development of bulbar palsy. For the next 4 years, there were no apparent neurological changes, and the patient's state remained stable with continued tube feeding. In the final year of his life, the patient presented with respiratory failure due to central alveolar hypoventilation on three occasions. The patient became comatose and died after a total disease duration of 11 years. The patient was not placed on mechanical ventilation. No apparent cognitive dysfunction was prior to death.

Materials and methods

Neuropathological analysis

An autopsy of the brain and spinal cord was performed, and the tissue was fixed in 10% formalin. Neuropathological examinations were performed on 8 μm thick sections using hematoxylin-eosin, Klüver-Barrera, Bodian, Gallyas-Braak, and Holzer staining. Immunostaining for anti-GFAP antibody (DAKO, Glostrup, Denmark; mouse monoclonal, diluted 1 400), anti-αB crystallin antibody (Novocastra, Newcastle upon Tyne, UK, rabbit polyclonal, diluted 1 1,000), anti-neurofilament antibody (DAKO, mouse monoclonal, diluted 1 400), anti-CD45 antibody (DAKO, mouse monoclonal, diluted 1 100), and anti-CD68 antibody (DAKO, mouse monoclonal, diluted 1 100) was also carried out as appropriate. Primary antibody binding was detected by the labeled streptavidin-biotin method (Dako LSAB kit; DAKO). Peroxidase-conjugated streptavidin was visualized with 3,3'-diaminobenzidine (DAB; Wako Pure Chemical Industries,

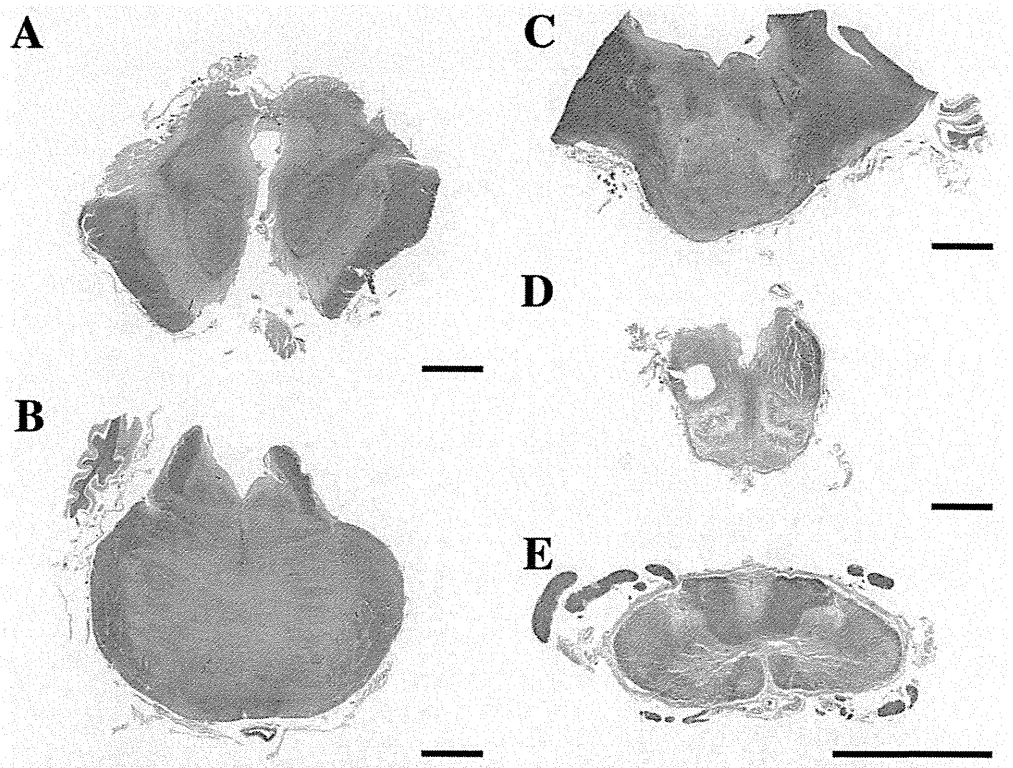

Figure 2. Loupe images of the brainstem and cervical cord. A: The midbrain shows no apparent atrophy, and the cerebellar peduncle is preserved. B: The upper pons shows myelin pallor in the pontine base. The superior cerebellar peduncles are preserved. C: The lower pons shows atrophy of the pontine base with myelin pallor. The middle cerebellar peduncles are preserved. D: The medulla oblongata shows severe atrophy with myelin pallor. E: The cervical cord shows myelin pallor in the anterolateral column and fasciculus gracilis. Scale bars: 5 mm; Klüver-Barrera staining.

Osaka, Japan) as the chromogen. Immunostained sections were counterstained lightly with Mayer's hematoxylin.

The morphological study of mutant GFAP

To clarify the effects of the mutant GFAP, we experimentally examined the expression patterns of S393R compared with wild-type GFAP transfected in human adrenal carcinoma-derived cells (SW13 cells) by immunofluorescence. Details of the morphological and functional studies including the methods for quantitation and the SW13 cell line that was used were described previously [5, 6].

Results

Macroscopic appearance

At autopsy, the brain weighed 1,380 g and showed no apparent cerebral atrophy. In coronal sections of the cerebrum, the anterior horns of the lateral ventricles showed mild dilatation, but no abnormalities were observed in the cerebral cortex and white matter, basal ganglia, or thalamus. The hippocampal formation was also well preserved. The cerebellum, including the dentate nucleus, showed no apparent abnormality. On axial sections of the brainstem, the midbrain and upper pons were preserved from atrophy, whereas the lower pons and medulla oblongata showed severe atrophy (Figure 2A, B, C, D). The medulla oblongata showed gelatinous degeneration. There was no apparent depigmentation in the substantia nigra or locus ceruleus. The spinal cord showed general atrophy, particularly in the cervical cord, but the anterior and posterior nerve roots were preserved from atrophy.

Microscopic appearance

The cerebral cortex, including the hippocampus, showed no apparent abnormalities.

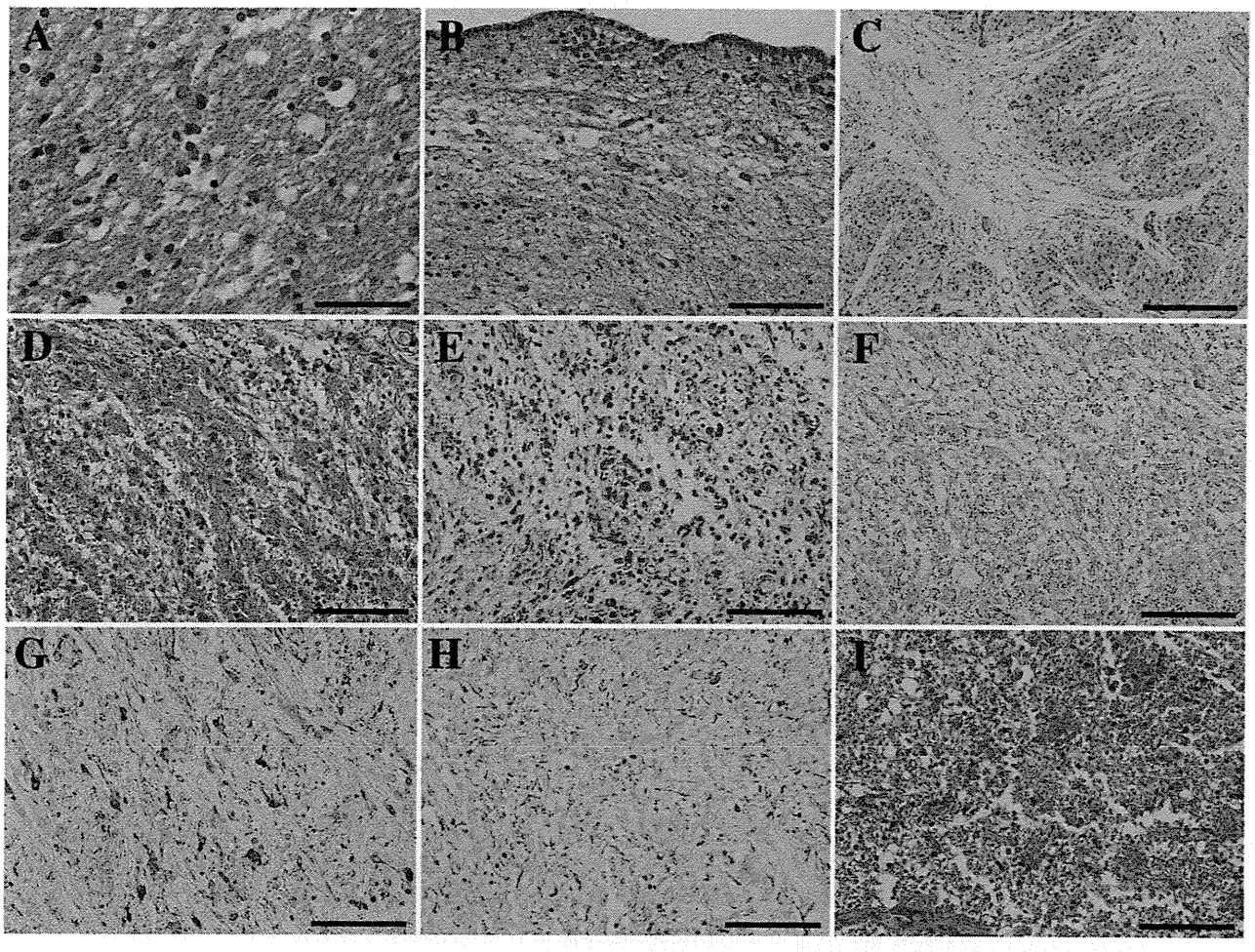

Figure 3. Representative microscopic images of the brain. A: A few Rosenthal fibers are observed in the cerebral white matter (occipital lobe, hematoxylin and eosin (H&E) staining). B: In the cerebellar white matter, Rosenthal fibers are recognized in small numbers (subependymal tissue of the 4th ventricle, H&E staining). C: The inferior olivary nucleus shows severe tissue rarefaction and myelin loss, whereas the neurons are relatively preserved in number (Klüver-Barrera (K&B) staining). D-G: The tegmentum of the medulla oblongata shows numerous Rosenthal fibers. The Rosenthal fiber shows a thick and eosinophilic bundle by H&E staining (D) and an elongated and blue colored bundle by K&B staining (E). The Rosenthal fiber shows immunopositive findings by anti-GFAP (F) and anti-αB crystallin immunostaining (G). H: Anti-neurofilament immunostaining shows relatively preserved axons in the degenerative region (tegmentum of the medulla oblongata). I: The cervical cord shows numerous Rosenthal fibers (H&E staining). Scale bars: A: 50 μm; B, D, E, F G, H, I: 100 μm; C: 500 μm.

A few Rosenthal fibers were observed in the cerebral white matter, basal ganglia, thalamus, and cerebellum, particularly in the ventricular subependymal tissue (Figure 3A, B), but were not so apparent in the perivascular regions. Reactive astrocytes were not apparent in the supratentorial tissues and cerebellum. In the midbrain, the substantia nigra, red nucleus, and oculomotor nerve nucleus were preserved from neuron loss, and the cerebral peduncles were well preserved from myelin loss. In the pons, the pontine nucleus, locus ceruleus, abducens nerve nucleus, and facial nerve nucleus showed gliosis but were preserved from neuron loss. The longitudinal and transverse pontine fibers showed myelin loss particularly in the lower pons but were preserved from axon loss. Numerous Rosenthal fibers were extensively observed from the middle of the pons to the cervical cord (Figure 3D, E, F, G, H, I). In the medulla oblongata, the tegmentum and pyramid showed severe degeneration with myelin loss, but the axons were relatively preserved. The medial longitudinal fasciculus, tectospinal tract, and medial lemniscus were relatively preserved from the myelin loss. The borderline of the myelin loss was indistinct. The inferior olivary nucleus and hypoglossal nerve nucleus showed severe tissue rarefaction and my-

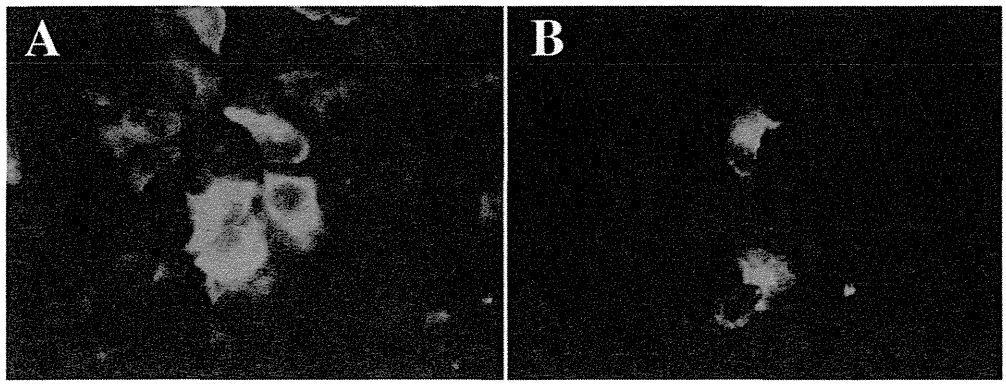

Figure 4. Immunofluorescence of astrocytes with wild-type and S393R *GFAP* gene mutation. The expression patterns in astrocytoma-derived cells (SW13 cells) stained with polyclonal antibody for GFAP (green color) between cells transfected with wild-type GFAP and cells transfected with S393R mutant *GFAP* gene. A: Cells transfected with wild-type GFAP. A filamentous pattern, which cannot be distinguished from a normal appearing filamentous GFAP structure, is observed. Polarized distribution pattern shows polar distribution of GFAP in mitosis. B: Cells transfected with S393R mutant *GFAP* gene. Filamentous pattern shows an aggregate or amorphous pattern, which shows irregular aggregation of GFAP with a few filamentous structures or the appearance of cells in which the filament networks are destroyed. Magnification: 40×.

elin loss, whereas the neurons were relatively preserved in number (Figure 3C). In the severely affected regions of the medulla oblongata and cervical cord, no apparent reactive astrocytes were observed, and GFAP-positive astrocytes were decreased in number. By LCA immunostaining, mild positive lymphocyte infiltration was observed, but no apparent positive microglia infiltration was observed by CD68 immunostaining. The superior, middle, and inferior cerebellar peduncles were preserved from myelin loss. In the spinal cord, myelin pallor was observed in the anterolateral column and fasciculus gracilis (Figure 2E). Macrophages were observed in the lateral corticospinal tract and posterior column due to Waller degeneration. The number of anterior motor neurons was relatively preserved. The anterior and posterior nerve roots were preserved from myelin loss and axon loss. In regard to aging-related pathology, a few neurofibrillary tangles (Braak stage I) were observed in the transentorhinal cortex. Senile plaques, Lewy bodies, and vascular lesions were not observed.

Functional alteration of mutant GFAP

A morphological change of GFAP was found in SW 13 cells transfected with the S393R *GFAP* mutation. The cells transfected with wild-type GFAP showed a filamentous pattern (Figure 4A) indistinguishable from a normal-appearing filamentous GFAP structure. However, the cells transfected with the S393R mutant *GFAP* gene showed an aggregate or amorphous filamentous pattern, with either a few filamentous structures or the appearance of cells in which the filament networks were destroyed (Figure 4B). Compared to the wild-type cells, the aggregates were found in the perinuclear region, and the filamentous structures were decreased in number.

Discussion

Although MRI findings, such as extensive white matter changes with frontal predominance and periventricular rim observed in the cerebral form or severe atrophy of the medulla oblongata to the cervical cord observed in the bulbospinal form, can clinically assist in the diagnosis of Alexander disease, this disease can be definitively diagnosed by *GFAP* gene analysis or pathological examination [1, 2, 3]. Alterations of the *GFAP* gene have been reported in 90%, but not 100%, of Alexander disease cases that underwent analysis [1, 2, 3, 6]. To date, more than 100 GFAP gene mutations including point mutations, deletions, frame shifts, or aberrant splicing have been reported in patients with Alexander disease [1, 2], the majority of which are identified as point mutations in the coding region of the *GFAP* gene [1, 2]. Fol-

lowing the identification of the *GFAP* gene mutations in the patients with Alexander disease, milder forms of the disease with juvenile or adult onset have been described with increasing frequency, and the phenotypes of Alexander disease seem to have increased [1, 2]. In the present case, *GFAP* gene analysis revealed a point mutation of S393R, which is currently not reported in the Alexander disease database [2].

Although *GFAP* gene mutation in many patients with Alexander disease is not inherited from the parents but occurs spontaneously [2], 65% of patients with the bulbospinal form of Alexander disease have a family history of the disease [1, 4]. However, the hot spots of GFAP mutations in bulbospinal-form Alexander disease have not been identified [1, 4]. Although the present case corresponded clinicopathologically to the bulbospinal form, no apparent family history was recognized; thus, this case may be due to a de novo mutation.

Because the *GFAP* gene mutation was discovered in cases of Alexander disease, experimental research was conducted to determine the relation between each mutation and the pathologic findings in addition to the clinical presentation [1, 2, 3]. Although the investigations on aggregate formation in *GFAP* gene mutations concluded that the mutations decrease the solubility of GFAP [1, 3], the relation between genotypes and phenotypes in Alexander disease remains unclear [1, 2, 3, 7].

In immunohistochemical and immunofluorescence studies using astrocytoma-derived cells, most mutant GFAP cells showed a filamentous pattern indistinguishable from normal GFAP cells; however, some mutant GFAP cells are known to show an irregular aggregation with few filamentous structures or appear as cells where filament networks are destroyed [1, 5, 6]. In the present investigation, we performed an experimental study using cultured cells transfected with the mutation suggesting a potential mechanism and obtained findings of abnormal GFAP aggregation similar to those with the S393R mutation. In the cells transfected with the S393R mutant *GFAP* gene, an aggregate or amorphous filamentous pattern was observed, with either irregular aggregation of GFAP with a few filamentous structures or the appearance of cells in which the filament networks were destroyed. According to cell and animal model experiments, formation of the mutant GFAP aggregate depends on the site of the GFAP mutation [1], and Alexander disease pathology involves not only functional abnormalities in the intermediate filaments but also functional abnormalities in the astrocytes and neurons [1, 5, 6]. Furthermore, it is possible that polymorphism in the GFAP promoter gene regulates the degree to which GFAP is expressed. This may have an effect on clinical heterogeneity [1], and the severity of pathological changes of cerebral white matter may be determined by certain factors related to each glial developmental stage [1, 4].

In the severely damaged areas in the medulla oblongata and cervical cord, even though the myelin sheaths were severely affected, the axons were relatively well preserved. Although this pathological change can be regarded as a form of demyelination or dysmyelination, we could find no apparent pathological alterations in the oligodendroglia. In general, the pathology of Alexander disease shows destruction of the white matter with Rosenthal fibers in the glia limitans and periventricular areas [2, 8]. The filaments of the Rosenthal fibers contain GFAP, αB crystallin, heat shock protein 27, and ubiquitin, but not vimentin [1, 2, 3, 9]. In the present case, GFAP-positive astrocyte was decreased in number and no apparent reactive astrocyte was observed in the severely affected regions of the medulla oblongata and cervical cord.

Salmaggi et al. [10] described a 35-year-old Italian woman with adult-onset Alexander disease with the same codon 393 mutation of the *GFAP* gene [2]. That case showed an S393I (not S393R) GFAP mutation. The patient presented with a 2-year history of progressive lower paraparesis, dysarthria, and dysphagia [10]. Neurological examinations showed dysphagia, pseudobulbar speech, and hyperreflexia with Babinski sign [10]. MRI showed T_2-hyperintensity in the bulbar tegmentum, olivary nucleus, superior cerebellar peduncles, dentate nucleus, and frontal periventricular white matter, with slight cervical cord atrophy [10]. The patient's mother had died at 49 years after a similar 15-year neurological disease [10]. The clinical findings were similar, in part, to